Aberrant dolichol chain lengths as biomarkers for retinitis pigmentosa caused by impaired dolichol biosynthesis

Rong Wen,[1,2,*] Byron L. Lam,[1,2,*] and Ziqiang Guan[1,2,†]

Bascom Palmer Eye Institute,* University of Miami Miller School of Medicine, Miami, FL 33136; and Department of Biochemistry,† Duke University Medical Center, Durham, NC 27710

Abstract We observed a characteristic shortening of plasma and urinary dolichols in retinitis pigmentosa (RP) patients carrying K42E and T206A mutations in the *dehydrodolichol diphosphate synthase* (*DHDDS*) gene, using liquid chromatography-mass spectrometry. Dolichol-18 (D18) became the dominant dolichol species in patients instead of dolichol-19 (D19) in normal individuals. The D18/D19 ratio was calculated and used as an index of dolichol length distribution. K42E/K42E and K42E/T206A patients have significantly higher plasma and urinary D18/D19 ratios than K42E and T206A carriers. The ratios of carriers are significantly higher than normal individuals. Receiver operating characteristic (ROC) analysis shows that plasma and urinary D18/D19 ratios can unambiguously discriminate patients from carriers, and carriers from normal individuals. Dolichol analysis also provides evidence that the T206A mutation is RP-causative. The methodologies and procedures used for dolichol profiling are reliable, high throughput, and cost effective. Dolichol profiling, complementary to genotyping, can be readily adapted as a test in the clinic not only for the diagnosis of patients but also for identification of carriers with DHDDS or other genetic mutations that may impair dolichol biosynthesis.— Wen, R., B. L. Lam, and Z. Guan. **Aberrant dolichol chain lengths as biomarkers for retinitis pigmentosa caused by impaired dolichol biosynthesis. *J. Lipid Res.* 2013.** 54: **3516–3522.**

Supplementary key words dehydrodolichol diphosphate synthase • autosomal recessive • dolichol-18:dolichol-19 ratio • mass spectrometry • human blood • human urine

Dolichols are long chain polyisoprenoid alcohols mainly composed of 17-21 isoprene units in mammalian cells (1, 2). Discovered more than 50 years ago (3, 4), the biological functions of free dolichols are still not understood, although dolichol phosphate, the phosphorylated derivative of dolichol, is known to be the obligate lipid carrier for *N*-linked protein glycosylation (5–10). As a *cis*-prenyltransferase and a key enzyme in dolichol biosynthesis (5, 11), dehydrodolichol diphosphate synthase (DHDDS) assembles chains of five-carbon isoprene units through a prenyl chain elongation process into linear polyprenyl diphosphate with predetermined lengths, which subsequently undergo dephosphorylation and reduction of the α-isoprene unit to form dolichols (5, 12). In human, dolichol-19 (D19, containing 19 isoprene units) is the most abundant species (1, 2).

We recently identified a single-nucleotide c.124A>G mutation in the dehydrodolichol diphosphate synthase-encoding *DHDDS* gene that changes the highly conserved Lys42 to Glu (K42E) as the cause of autosomal recessive retinitis pigmentosa (arRP) in a family of Ashkenazi Jewish (AJ) origin (13). The same mutation was subsequently confirmed as the cause of RP in 12% of arRP patients of AJ origin and is found heterozygously in 1 out of 322 in the AJ population (14). RP is a heterogeneous group of hereditary retinal degenerative disorders affecting 1 in 3,000–4,500 with no effective treatments available (15–17). Mutations in more than 60 genes are implicated in RP, including in nearly 50% of arRP cases (15–17).

To assess the biochemical and physiological consequences of the K42E DHDDS mutation on dolichol biosynthesis, we characterized dolichols in urine and plasma samples from patients and carriers by liquid chromatography-mass spectrometry (LC-MS). Here we report that dolichols in patients homozygous for the K42E mutation are characteristically shorter than those in normal individuals. As a result, D18 becomes the dominant species. Dolichols of carriers are shortened, although to a lesser extent. Shortened dolichol profile was also found in a patient carrying the compound heterozygous T206A/K42E mutations in the *DHDDS* gene. Our results indicate that plasma and urinary dolichol profiles are functional readouts of dolichol biosynthesis and can serve as biomarkers for diagnosis of arRP and perhaps other diseases caused by abnormal dolichol biosynthesis and metabolism.

This work was supported by National Institutes of Health Grants R01 EY-018586 and P30 EY-014801; LIPID MAPS Collaborative Grant GM-069338; Department of Defense Grant W81XWH-09-1-0674; Adrienne Arsht Hope for Vision, and an unrestricted grant from Research to Prevent Blindness, Inc.

Manuscript received 19 August 2013 and in revised form 23 September 2013.

Published, JLR Papers in Press, September 27, 2013
DOI 10.1194/jlr.M043232

Abbreviations: arRP, autosomal recessive RP; DHDDS, dehydrodolichol diphosphate synthase; MRM, multiple reaction monitoring; ROC, receiver operating characteristic; RP, retinitis pigmentosa; WT, wild-type.

[1] R. Wen, B. L. Lam, and Z. Guan contributed equally to this work.
[2] To whom correspondence should be addressed.
e-mail: ziqiang.guan@duke.edu (Z.G.); blam@med.miami.edu (B.L.L.); rwen@med.miami.edu (R.W.)

MATERIALS AND METHODS

Sample collection

This study was approved by the Institutional Review Board of the University of Miami (protocol number 20110767). All participants provided written informed consent. Sample collection was untimed and without restrictions, including diet and liquid intake. Blood was collected in Vacutainer plasma preparation tubes (PPT) (5 ml capacity, BD, Franklin Lakes, NJ), spun at 1,300 *g* for 10 min. Plasma was obtained and stored at −80°C. Off-site plasma samples were collected by designated labs in the vicinity of residences of the individuals and shipped at ambient temperature via express carriers to the Bascom Palmer Eye Institute in Miami, FL.

Urine samples (20–30 ml) were collected in 50 ml tubes containing sodium azide (~0.02% final concentration) and stored at −80°C. Sample collection kits were provided to individuals for off-site collection at their residences. Samples were shipped at ambient temperature via express carriers to the Bascom Palmer Eye Institute.

Lipid extraction

Lipid extraction was done following a modified Bligh and Dyer method (18). Briefly, plasma (0.3 ml) was mixed with methanol (0.3 ml) on a Bullet Blender (Next Advance, Averill Park, NY) for 2 min. Chloroform (0.3 ml) was then added and mixed again for 2 min. Samples were subsequently centrifuged for 10 min, and the lower chloroform layer containing lipids was transferred to a new tube. Lipids (in chloroform) were dried for 2 h or overnight on a SpeedVac (Savant Instruments, Holbrook, NY), flushed with argon, and stored at −20°C. For urinary samples, 3 ml of urine was mixed with 3 ml of methanol by vortexing for 1 min. Chloroform (1.5 ml) was added and vortexed again for 1 min. The sample was then centrifuged for 10 min, and the lower chloroform layer was transferred to a new tube. Lipids were dried on a SpeedVac, flushed with argon, and stored at −20°C, as described above. Dried lipids were shipped via express carriers at ambient temperature to Duke University in Durham, NC for dolichol analysis.

LC-MS analysis of dolichols

Dolichols were analyzed by LC-MS (19) performed in multiple reaction monitoring (MRM) mode using a Shimadzu LC system (comprising a solvent degasser, two LC-10A pumps, and a SCL-10A system controller) coupled to a 4000 Q-Trap hybrid triple quadrupole linear ion-trap mass spectrometer equipped with a Turbo V ion source (AB-Sciex, Foster City, CA). LC was operated at a flow rate of 200 μl/min with a linear gradient as follows: 100% of mobile phase A was held isocratically for 2 min, and then linearly increased to 100% mobile phase B over 14 min, and held at 100% B for 4 min. Mobile phase A consisted of methanol/acetonitrile/aqueous 1 mM ammonium acetate (60/20/20, v/v/v). Mobile phase B consisted of 100% ethanol containing 1 mM ammonium acetate. A Zorbax SB-C8 reversed-phase column (5 μm, 2.1 × 50 mm) was obtained from Agilent.

MRM was performed in the negative ion mode with MS settings as follows: curtain gas (CUR) = 20 psi (pressure); gas-1 (GS1) = 20 psi; gas-2 (GS2) = 30 psi; ion spray (IS) voltage = −4500 V; source temperature (TEM) = 350°C; interface heater = ON; declustering potential (DP) = −40V; entrance potential (EP) = −10V; and CXP = −5V. The voltage used for collision-induced dissociation was −40V (laboratory frame of energy). Nitrogen was used as the collision gas. The MRM pairs for D17, D18, D19, and D20 were 1236.2/59, 1304.2/59, 1372.2/59, and 1440.3/59, respectively. In these MRM pairs, the precursor ions are the $[M+acetate]^-$ adduct ions, and the product ions are the acetate ions (*m/z* 59).

Statistical analysis

All statistical analyses, including *t*-test, ANOVA, and receiver operating characteristic (ROC) curve analysis, were performed using IBM SPSS Statistics software (IBM, Armonk, NY). Significant

TABLE 1. Demographics, DHDDS genotypes, and D18/D19 ratios in plasma and urine

Variable	arRP Patients with DHDDS Mutations (n = 9)	Carriers of DHDDS Mutations (n = 35)	arRP Patients with WT DHDDS (n = 34)	Normal Individuals (n = 19)
Gender				
Male	5	13	18	11
Female	4	22	16	8
Mean age in years (range)	43.2 (34–55)	46.1 (8–89)	42.6 (14–75)	43.1 (8–60)
Race[a]				
White	9	35	31	13
Other	0	0	3	6
Ashkenazi Jewish ethnicity[a]	9	35	1	8
DHDDS mutation				
K42E	8	30		
T206A		5		
K42E/T206A	1			
Plasma D18/D19 ratio[b]				
WT			0.84 ± 0.10 (n = 34)	0.82 ± 0.12 (n = 16)
K42E	2.84 ± 0.38 (n = 8)	1.56 ± 0.11 (n = 25)		
T206A		1.31 ± 0.06 (n = 5)		
K42E/T206A	2.59 (n = 1)			
Urinary D18/D19 ratio[b]				
WT			0.46 ± 0.02 (n = 6)	0.47 ± 0. 06 (n = 13)
K42E	4.00 ± 0.45 (n = 8)	1.27 ± 0.09 (n = 30)		
T206A		1.04 ± 0.04 (n = 5)		
K42E/T206A	3.39 (n = 1)			

[a] Race and ethnicity were self-reported.
[b] Data are presented as mean ± SD.

differences in the mean values between groups were analyzed by Student *t*-test for two groups or by ANOVA (ANOVA) and Tukey test for more than two groups. Data are presented as mean ± SD. Cutoff levels were selected from the table of ROC curve coordinates to obtain the highest sensitivity and specificity.

RESULTS

The demographics, DHDDS genotypes, and dolichol profiling data of all study subjects are summarized in **Table 1**.

Plasma and urinary dolichol profiles in a family with the K42E DHDDS mutation

The structure of dolichol is shown in **Fig. 1A**. Plasma and urine dolichols from members of Family A, in which the K42E DHDDS mutation was first discovered (13) (Fig. 1B), were characterized. In the three affected siblings, dolichol profiles are consistently shorter (by about one isoprene unit) than that of the unaffected sibling who has the wild-type (WT) DHDDS. In the affected individuals, D18 became the dominant dolichol species (Fig. 1C). The profiles

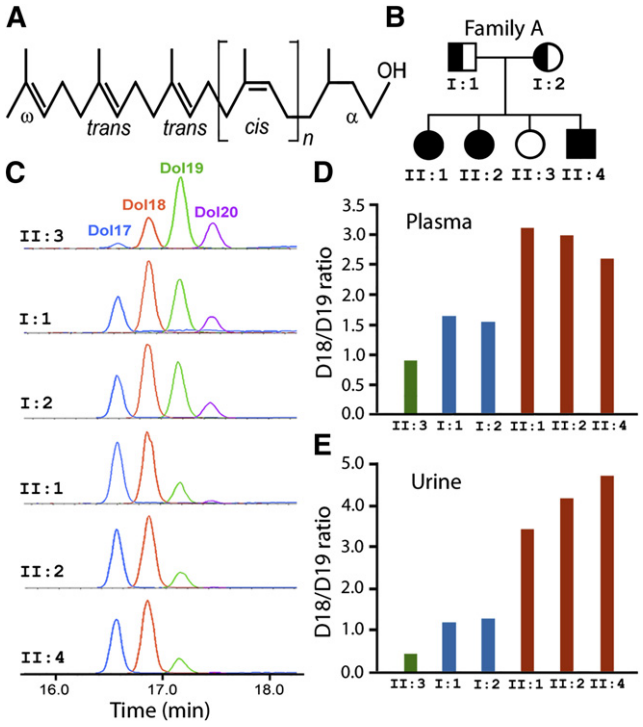

Fig. 1. Plasma and urinary dolichol profiles of Family A. (A) Structure of dolichols. Dolichols are long-chain polyisoprenoid alcohols with a saturated α-isoprene unit and two *trans* units at the ω-end. (B) Pedigree of Family A. Three of the four siblings are homozygous for the K42E DHDDS mutation and were diagnosed with RP. (C) LC-MRM chromatograms of urinary dolichol profiles of all six family members. Dolichol profiles of those with K42E/K42E genotype are shortened, and D18 [II:1, II:2, and II:4 (orange)] becomes the dominant dolichol instead of D19 [II:3 (green)]. (D and E) The D18/D19 ratios of the affected individuals (red bars) are much higher than that of the unaffected individual (green bars), whereas the ratios of the K42E carriers (blue bars) are lower than those of the patients but higher than the unaffected individuals. The separation of D18/D19 ratios among affected siblings, parents (carriers), and the unaffected sibling is greater in urine than in plasma.

of two carriers (parents) are longer than those of the affected individuals but shorter than that of the normal individual, suggesting that both the WT and mutant DHDDS proteins are functional (Fig. 1C).

We calculated D18/D19 ratio and used it as an index to quantitatively describe dolichol profile. The D18/D19 ratios of affected siblings are much higher than that of the unaffected sibling. Not surprisingly, D18/D19 ratios of carriers are lower than those of the affected siblings but higher than that of the unaffected sibling (Fig. 1C, E). The separations in the D18/D19 ratios among the affected individuals, carriers, and unaffected individual are greater in urine than in plasma (Fig. 1D, E).

Plasma and urinary D18/D19 ratios in arRP patients with the K42E mutation, in carriers, and in normal individuals

To further confirm the characteristic changes in dolichol profile, we collected and analyzed plasma samples from 6 K42E/K42E patients, 25 K42E carriers, and 16 normal individuals. The mean plasma D18/D19 ratio of K42E/K42E patients (2.75 ± 0.28, mean ± SD, n = 6) is 3.4 times higher than that of the normal individuals (0.82 ± 0.12, n = 16, $P < 0.001$), and 1.8 times higher than the ratio of K42E carriers (1.56 ± 0.11, n = 25, $P < 0.001$) (**Fig. 2A**). The mean plasma ratio of K42E carriers is 1.9 times higher than that of the normal individuals ($P < 0.001$) (Fig. 2A). The narrow distribution of the D18/D19 ratios in the carriers and normal individuals (Fig. 2A) indicates that the plasma D18/D19 ratios are not appreciably influenced by age, gender, or time of collection, as sample collections were untimed and without restrictions (see Materials and Methods).

ROC curve analysis shows that the plasma D18/D19 ratio discriminates K42E/K42E patients from K42E carriers with an area under curve (AUC) of 1.0 and 100% sensitivity and specificity at the cutoff level of 2.14 (Fig. 2B). The D18/D19 ratio also discriminates K42E carriers from normal individuals with an AUC of 1.0 and 100% sensitivity and specificity at the cutoff level of 1.14 (Fig. 2C).

Urinary samples were analyzed in 6 K42E/K42E patients, 30 K42E carriers, and 13 normal individuals. The mean urinary D18/D19 ratio of K42E/K42E patients (4.10 ± 0.44, mean ± SD, n = 6) is 8.7 times higher than normal individuals (0.47 ± 0. 06, n = 13, $P < 0.001$), and 3.2 times higher than K42E carriers (1.27 ± 0.09, n = 30, $P < 0.001$) (Fig. 2D). The mean urinary D18/D19 ratio of K42E carriers is 2.7 times higher than normal individuals ($P < 0.001$) (Fig. 2D). As in the plasma, distribution of the D18/D19 ratios in the urine of carriers and normal individuals (Fig. 2A) is very narrow, indicating that the urinary D18/D19 ratios are not significantly influenced by age, gender, or timing of collection, as sample collections were untimed and without restrictions (see Materials and Methods). Of note, the separation of D18/D19 ratios among the three groups (K42E/K42E patients, K42E carriers, and normal individuals) in urine is higher than that it is in plasma.

ROC curve analysis indicates that the urinary D18/D19 ratio discriminates K42E/K42E patients from K42E carriers with an AUC of 1.0 and 100% sensitivity and specificity at the

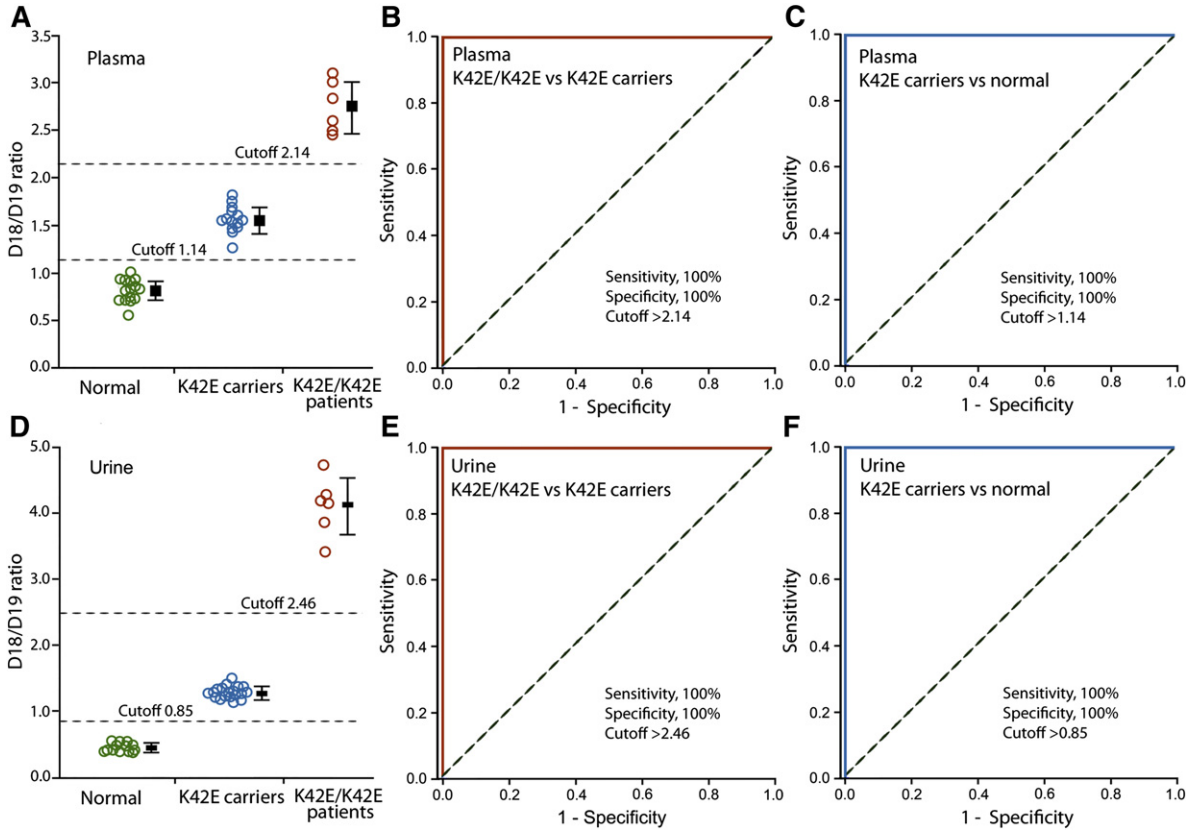

Fig. 2. Plasma and urinary D18/D19 ratios in K42E/K42E patients, K42E carriers, and normal individuals. Plasma dolichol profiling was performed on 6 K42E/K42E patients, 25 K42E carriers, 16 normal individuals (A). ROC curve analysis shows that plasma D18/D19 ratios discriminate patients from carriers with 100% sensitivity and specificity (B), and carriers from normal individuals with 100% sensitivity and specificity (C). Urinary dolichol profiling was performed on 6 K42E/K42E patients, 30 K42E carriers, and 13 normal individuals (D). Urinary D18/D19 ratios also discriminate patients from carriers with 100% sensitivity and specificity (E), and carriers from normal individuals with 100% sensitivity and specificity (F). A bar representing the mean D18/D19 ratio (± SD) of each group is next to the plotted data (A and D). D18/D19 ratios are well separated among the three genotypic groups, with the separation being greater in urine than in plasma. The dotted diagonal lines indicate a reference line of AUC = 0.5 (B, C, E, and F).

cutoff level of 2.46 (Fig. 2E). The D18/D19 ratio in urine also discriminates K42E carriers from normal individuals with an AUC of 1.0 and 100% sensitivity and specificity at the cutoff level of 0.85 (Fig. 2F).

Plasma and urinary D18/D19 ratios distinguish arRP patients carrying the K42E DHDDS mutation from arRP patients with wild-type DHDDS

To demonstrate the predictive value of the D18/D19 ratio as a biomarker for dolichol metabolism and for the diagnosis of arRP caused by abnormal dolichol metabolism, we blindly screened plasma samples from 36 arRP patients that had been collected at the Bascom Palmer Eye Institute since 2008. The genetic mutations of these patients were not identified previously. Two patients (from the same family) were found to have high D18/D19 ratios of 2.66 and 3.59, above the cutoff level of 2.14 for K42E/K24E patients (**Fig. 3A**). Their urinary D18/D19 ratios are 3.45 and 3.93, also above the cutoff level of 2.46 for homozygous K42E mutation (Fig. 3B). Subsequent genotyping confirmed that both are homozygous for the K42E DHDDS mutation.

Dolichol profiles of the remaining 34 arRP patients are all in the normal range. The mean plasma D18/D19 ratio was 0.84 ± 0.10 (mean ± SD, n = 34), indistinguishable from that of normal individuals (0.82 ± 0.12, n = 16, P = 0.60) (Fig. 3A). Urinary samples were recently collected from 6 of these patients. Their mean urinary D18/D19 ratio is 0.46 ± 0.02 (n = 6), indistinguishable from that of normal individuals (0.47 ± 0.06, n = 13, P = 0.51) (Fig. 3B). Together, these results demonstrate that plasma and urinary D18/D19 ratios can reliably distinguish arRP patients homozygous for the K42E DHDDS mutation from arRP patients with WT DHDDS.

Dolichol profiles of an arRP patient with compound heterozygous K42E/T206A DHDDS mutations

A single base c.616 A>G mutation in the DHDDS-encoding gene that changes Thr206 to Ala was recently discovered in a patient (Family B, **Fig. 4A**) with compound heterozygous K42E/T206A DHDDS mutations. Because this is the first RP patient identified to have the T206A mutation and because he is heterozygous for the T206A allele, whether the T206A mutation was RP-causative needed to be determined.

This question was addressed by dolichol analysis. The patient's urinary D18/D19 ratio is 3.39, and his plasma D18/D19 ratio is 2.59. Both are above the cutoff levels for

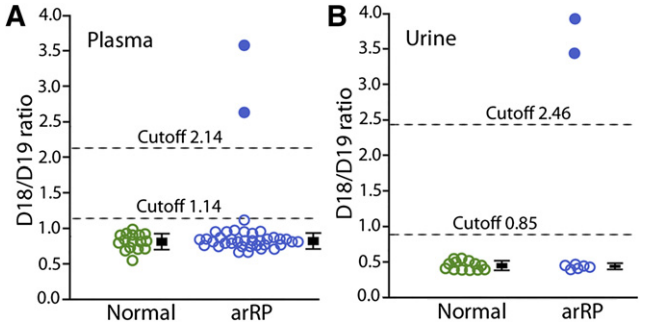

Fig. 3. Plasma and urinary dolichol profiles of arRP patients with unknown genotypes. Dolichol profile was analyzed with samples from 36 arRP patients whose genetic mutations were not previously identified. Two patients were found to have high plasma D18/D19 ratios of 2.66 and 3.59 (A, blue dots) and urinary ratios of 3.45 and 3.93 (B, blue dots), well above the plasma and urinary cutoff levels for K42E/K42E patients. Plasma D18/D19 ratios of the other 34 patients (A, blue circles) and the urinary D18/D19 ratios of the other 6 arRP patients (B, blue circles) are in the normal range. Plasma data from 16 normal individuals (A, green circles) and urine data from 13 normal individuals (B, green circles) are presented for comparison. A bar representing the mean D18/D19 ratio (± SD) of each group is next to the plotted data. Data of patients above the cutoff line are not included in the arRP groups.

K42E/K42E patients (Fig. 4B, C). The high D18/D19 ratios could have two possible interpretations. First, the T206A mutation could be a null-equivalent lost-of-function mutation so that the high D18/D19 ratio was solely determined by the K42E allele. Alternatively, the T206A DHDDS mutant could be functionally similar to the K42E mutant and, therefore, contributed to the high D18/D19 ratios. To resolve this issue, samples from the parents were analyzed. Their urinary D18/D19 ratios are 1.12 and 1.07, both above the cutoff level of 0.85 for K42E carriers. Their plasma D18/D19 ratios are 1.55 and 1.36, respectively, also above the cutoff level of 1.13 for K42E carriers (Fig. 4C). Results from the parents strongly indicate that each parent carries a K42E-equivalent mutation. Since one parent is an obligate T206A carrier, the high D18/D19 ratios of both parents provide the first evidence that the T206A mutation affects dolichol biosynthesis in a manner similar to the K42E mutation. Thus the T206A mutation should be as RP-causative as the K42E mutation. Subsequent genotyping showed that the father carries the K42E mutation, and the mother has the T206A mutation (Fig. 4A). Five other family members also have D18/D19 ratios above the cutoff levels for carriers of DHDDS mutations (Fig. 4A–C). Genotyping identified one sibling is a carrier of the K42E mutation, and the other sibling and all three offspring are carriers of the T206A mutation.

DISCUSSION

The present work demonstrates clearly that dolichol profiles, presented as D18/D19 ratios, completely correlate with DHDDS genotypes. Dolichol profiling offers a unique advantage over genotyping in that it directly reveals the functional state of dolichol metabolism. This advantage

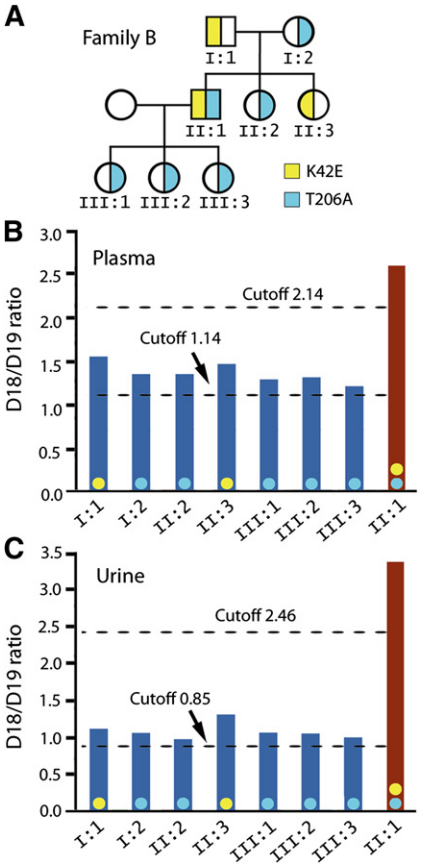

Fig. 4. Dolichol profiles of Family B with an arRP patient carrying compound heterozygous K42E/T206A mutations. Plasma and urinary D18/D19 ratios of this patient (A, II:1) are above the cutoff levels for K42E/K42E patients (B and C, red bars). Plasma and urinary D18/D19 ratios of seven other family members are all above the cutoff levels established for K42E carriers (B and C, blue bars). Genotyping subsequently revealed two family members as K42E carriers and five as T206A carriers (A). These data demonstrate that the T206A mutant is functionally defective in dolichol biosynthesis similar to the K42E mutant. Color-coded dots (yellow for K42E, light blue for T206A) are placed on each bar (B and C) to indicate genotypes.

became apparent when our dolichol profile data show conclusively that the T206A mutation is RP-causative. Our present work thus supports the notion that dolichol profiling can be used as a broad clinical test for detecting abnormal dolichol metabolism regardless of the cause, including known DHDDS mutations, as in the case of the T206A mutation, mutations yet to be identified, mutations in other genes that influence dolichol metabolism, such as the gene encoding the Nogo-B receptor necessary for DHDDS function (20), and epigenetic alterations that affect dolichol metabolism.

Dolichol length distribution is species-specific (21, 22). In humans, D19 is the most abundant dolichol (1, 2), whereas D18 is the most abundant dolichol in rat (23) and mouse (Z. Guan, B. L. Lam, and R. Wen, unpublished observations). Previous studies showed that mutations in the substrate-binding site of *cis*-prenyltransferase can dramatically influence dolichol lengths (24). The changes in dolichol length distribution we found in individuals homozygous

or heterozygous for the K42E DHDDS mutant are consistent with the hypothesis that the K42E mutation weakens substrate binding and lowers the efficiency of the enzyme (13).

The distribution of D18/D19 ratios in carriers or normal individuals is remarkably narrow and seemingly not influenced by age or gender. The D18/D19 ratio measurements tolerate fluctuations in the absolute amounts of dolichol in a sample, which could be influenced by diet, fluid intake, time of collection, and other factors. For the same reason, the D18/D19 ratio is less likely to be influenced by variations in sample processing and/or detection. In addition, free dolichols are unusually stable in biological samples. We found no appreciable changes in dolichol profiles (or D18/D19 ratios) in plasma or urinary samples stored at ambient temperatures for 30 days. Furthermore, dolichols are stable in lipid extracts. We routinely ship plasma and urinary samples, as well as extracted lipids, at ambient temperatures by overnight delivery service.

The greater separation of urinary D18/D19 ratios among patients, carriers, and normal subjects, as well as the ease and noninvasiveness of sample collection, makes urine a better clinical material for dolichol profiling. In blood, dolichols are associated with high-density lipoproteins (25–27), although the influence of such associations on the dolichol contents is unknown. The sources of urinary dolichols were not clearly identified. Dolichols have been detected in urine sediment and in whole urine (28, 29). However, we found significant amounts of dolichols in urinary liquid after urine samples were filtered with a 0.2 μm filter or centrifuged at 3,000 *g* for 10 min to remove cells and sediment, respectively.

Although the biological functions of free dolichol are not clearly understood (21, 30), the role of dolichol phosphate as an obligate lipid carrier for protein glycosylation is well established (10). Diseases related to DHDDS mutation are now considered as a type of congenital disorder of glycosylation (CDG) (31), a group of diseases caused by glycosylation deficiency (32, 33). Blood transferrin isoelectric focusing (IEF), which detects defective *N*-glycosylation of the protein, has been widely used as a biomarker for screening CDG. However, there are growing cases showing the limitations of this method (34). In fact, the three arRP patients of Family A showed normal blood transferrin IEF pattern. Therefore, plasma and urinary dolichol profiles may have the potential to serve as novel biomarkers for certain types of CDG caused by impaired dolichol biosynthesis.

It is unknown whether and how the shortened dolichol profiles in patients with DHDDS mutations contribute to the retinal degeneration phenotype. This important question could be potentially addressed in further studies using transgenic animals that carry DHDDS mutations identified in patients.

The LC/MS-based dolichol analysis is robust, high throughput, and cost effective. With appropriate automation in sample preparation, it is realistic that more than 100 samples could be analyzed per day. We believe blood and urinary dolichol profiling could be used as a first-line diagnostic test for identifying patients with abnormal dolichol metabolism or for carrier screening. Additionally, dolichol profiling could potentially serve as a surrogate biomarker for evaluating the efficacy of treatments aimed at rectifying abnormal dolichol metabolism.

The authors are grateful to patients and their families for participating in this study. The authors thank Drs. Yiwen Li and Potyra Rosa for technical assistance and discussion, Dr. Jerry Eichler for critically reading the manuscript, Dr. Timothy J. Schoen for discussion, and Mr. William J. Feuer for assistance in statistics.

REFERENCES

1. Quehenberger, O., A. M. Armando, A. H. Brown, S. B. Milne, D. S. Myers, A. H. Merrill, S. Bandyopadhyay, K. N. Jones, S. Kelly, R. L. Shaner, et al. 2010. Lipidomics reveals a remarkable diversity of lipids in human plasma. *J. Lipid Res.* **51:** 3299–3305.
2. Tollbom, O., and G. Dallner. 1986. Dolichol and dolichyl phosphate in human tissues. *Br. J. Exp. Pathol.* **67:** 757–764.
3. Pennock, J. F., F. W. Hemming, and R. A. Morton. 1960. Dolichol: a naturally occurring isoprenoid alcohol. *Nature.* **186:** 470–472.
4. Burgos, J., F. W. Hemming, J. F. Pennock, and R. A. Morton. 1963. Dolichol: a naturally-occurring C100 isoprenoid alcohol. *Biochem. J.* **88:** 470–482.
5. Schenk, B., F. Fernandez, and C. J. Waechter. 2001. The ins(ide) and out(side) of dolichyl phosphate biosynthesis and recycling in the endoplasmic reticulum. *Glycobiology.* **11:** 61R–70R.
6. Marquardt, T., and J. Denecke. 2003. Congenital disorders of glycosylation: review of their molecular bases, clinical presentations and specific therapies. *Eur. J. Pediatr.* **162:** 359–379.
7. Denecke, J., and C. Kranz. 2009. Hypoglycosylation due to dolichol metabolism defects. *Biochim. Biophys. Acta.* **1792:** 888–895.
8. Burda, P., and M. Aebi. 1999. The dolichol pathway of N-linked glycosylation. *Biochim. Biophys. Acta.* **1426:** 239–257.
9. Lehle, L., S. Strahl, and W. Tanner. 2006. Protein glycosylation, conserved from yeast to man: a model organism helps elucidate congenital human diseases. *Angew. Chem. Int. Ed. Engl.* **45:** 6802–6818.
10. Behrens, N. H., and L. F. Leloir. 1970. Dolichol monophosphate glucose: an intermediate in glucose transfer in liver. *Proc. Natl. Acad. Sci. USA.* **66:** 153–159.
11. Endo, S., Y. W. Zhang, S. Takahashi, and T. Koyama. 2003. Identification of human dehydrodolichyl diphosphate synthase gene. *Biochim. Biophys. Acta.* **1625:** 291–295.
12. Cantagrel, V., D. J. Lefeber, B. G. Ng, Z. Guan, J. L. Silhavy, S. L. Bielas, L. Lehle, H. Hombauer, M. Adamowicz, E. Swiezewska, et al. 2010. SRD5A3 is required for converting polyprenol to dolichol and is mutated in a congenital glycosylation disorder. *Cell.* **142:** 203–217.
13. Zuchner, S., J. Dallman, R. Wen, G. Beecham, A. Naj, A. Farooq, M. A. Kohli, P. L. Whitehead, W. Hulme, I. Konidari, et al. 2011. Whole-exome sequencing links a variant in DHDDS to retinitis pigmentosa. *Am. J. Hum. Genet.* **88:** 201–206.
14. Zelinger, L., E. Banin, A. Obolensky, L. Mizrahi-Meissonnier, A. Beryozkin, D. Bandah-Rozenfeld, S. Frenkel, T. Ben-Yosef, S. Merin, S. B. Schwartz, et al. 2011. A missense mutation in DHDDS, encoding dehydrodolichyl diphosphate synthase, is associated with autosomal-recessive retinitis pigmentosa in Ashkenazi Jews. *Am. J. Hum. Genet.* **88:** 207–215.
15. Hartong, D. T., E. L. Berson, and T. P. Dryja. 2006. Retinitis pigmentosa. *Lancet.* **368:** 1795–1809.
16. Heckenlively, J. R., S. L. Yoser, L. H. Friedman, and J. J. Oversier. 1988. Clinical findings and common symptoms in retinitis pigmentosa. *Am. J. Ophthalmol.* **105:** 504–511.
17. Pagon, R. A. 1988. Retinitis pigmentosa. *Surv. Ophthalmol.* **33:** 137–177.
18. Bligh, E. G., and W. J. Dyer. 1959. A rapid method of total lipid extraction and purification. *Can. J. Biochem. Physiol.* **37:** 911–917.
19. Guan, Z., and J. Eichler. 2011. Liquid chromatography/tandem mass spectrometry of dolichols and polyprenols, lipid sugar carriers across evolution. *Biochim. Biophys. Acta.* **1811:** 800–806.

20. Harrison, K. D., E. J. Park, N. Gao, A. Kuo, J. S. Rush, C. J. Waechter, M. A. Lehrman, and W. C. Sessa. 2011. Nogo-B receptor is necessary for cellular dolichol biosynthesis and protein N-glycosylation. *EMBO J.* **30:** 2490–2500.
21. Chojnacki, T., and G. Dallner. 1988. The biological role of dolichol. *Biochem. J.* **251:** 1–9.
22. Rush, J. S., S. Matveev, Z. Guan, C. R. Raetz, and C. J. Waechter. 2010. Expression of functional bacterial undecaprenyl pyrophosphate synthase in the yeast rer2{Delta} mutant and CHO cells. *Glycobiology.* **20:** 1585–1593.
23. Tavares, I. A., T. Coolbear, and F. W. Hemming. 1981. Increased hepatic dolichol and dolichyl phosphate-mediated glycosylation in rats fed cholesterol. *Arch. Biochem. Biophys.* **207:** 427–436.
24. Kharel, Y., S. Takahashi, S. Yamashita, and T. Koyama. 2006. Manipulation of prenyl chain length determination mechanism of cis-prenyltransferases. *FEBS J.* **273:** 647–657.
25. Elmberger, G., and P. Engfeldt. 1985. Distribution of dolichol in human and rabbit blood. *Acta Chem. Scand. B.* **39:** 323–325.
26. Elmberger, P. G., P. Engfeldt, and G. Dallner. 1988. Presence of dolichol and its derivatives in human blood. *J. Lipid Res.* **29:** 1651–1662.
27. Shiota, Y., K. Kiyota, T. Kobayashi, S. Kano, M. Kawamura, T. Matsushima, S. Miyazaki, K. Uchino, F. Hashimoto, and H. Hayashi. 2008. Distribution of dolichol in the serum and relationships between serum dolichol levels and various laboratory test values. *Biol. Pharm. Bull.* **31:** 340–347.
28. Bennett, M. J., N. J. Mathers, F. W. Hemming, I. Zweije-Hofman, and G. P. Hosking. 1985. Urinary sediment dolichol excretion in patients with Batten disease and other neurodegenerative and storage disorders. *Pediatr. Res.* **19:** 213–216.
29. Turpeinen, U. 1986. Liquid-chromatographic determination of dolichols in urine. *Clin. Chem.* **32:** 2026–2029.
30. Rip, J. W., C. A. Rupar, K. Ravi, and K. K. Carroll. 1985. Distribution, metabolism and function of dolichol and polyprenols. *Prog. Lipid Res.* **24:** 269–309.
31. Freeze, H. H. 2013. Understanding human glycosylation disorders: biochemistry leads the charge. *J. Biol. Chem.* **288:** 6936–6945.
32. Jaeken, J., and G. Matthijs. 2007. Congenital disorders of glycosylation: a rapidly expanding disease family. *Annu. Rev. Genomics Hum. Genet.* **8:** 261–278.
33. Freeze, H. H. 2006. Genetic defects in the human glycome. *Nat. Rev. Genet.* **7:** 537–551.
34. Mohamed, M., V. Cantagrel, L. Al-Gazali, R. A. Wevers, D. J. Lefeber, and E. Morava. 2011. Normal glycosylation screening does not rule out SRD5A3-CDG. *Eur. J. Hum. Genet.* **19:** 1019.